

# Effectiveness of High-Capacity Smoke Exhaust in Large Spaces

JAMES A. MILKE\*

*University of Maryland,  
College Park, MD, USA*

**ABSTRACT:** Current codes in many countries require that the smoke layer in an atrium or other large space be maintained above the highest means of egress in the space. The smoke exhaust capacity needed to maintain the smoke layer above the highest level of the means of egress can be substantial if that level is near the top of a tall atrium. However, the air entrained along the clear height of the plume that creates the vast quantity of smoke also acts to dilute the smoke. As such, a cost-effective design for an atrium smoke management system may be suggested that causes people to be exposed to the dilute smoke. The adequacy of such a design requires that the qualities of the remaining smoke layer be estimated. A first order analysis to estimate the properties of the smoke layer is described in this paper. Properties of interest include the concentration of gas species, visibility reduction and temperature. In some cases, the visibility may be reduced below 1 m even though the temperature rise and generation of toxic gases are relatively modest. However, with a smoke exhaust rate of 200 kg/s in an atrium, the hazard associated with the smoke layer temperature and CO concentration is modest for a wide range of fuels.

**KEY WORDS:** smoke management, atria, mechanical exhaust systems, smoke properties.

## INTRODUCTION

**I**N THE 1970's, the smoke exhaust capacity for atria and malls was stipulated by codes to be 4 to 6 air changes per hour. The basis of this requirement is commonly attributed to normal HVAC design for such spaces being 4 to 6 air changes per hour. Consequently, smoke management could be achieved using the normal HVAC fans, but in a different mode of operation. In the 1988 edition of the Life Safety Code [1], a requirement to restrict the descent of the smoke layer was stipulated for protected seating

---

\*E-mail: milke@eng.umd.edu

areas in assembly occupancies. As the NFPA Technical Committee on Smoke Management Systems initiated work on NFPA 92B in the mid-1980s, it became apparent that the volume-based air change per hour method of determining the smoke exhaust capacity did not relate to the provision of an equilibrium smoke layer position, such as alluded to in NFPA 101 in 1988 and later for covered malls and atria in NFPA 101 and model building codes [2]. In 1991, the first edition of NFPA 92B [3] presented a new design approach for the capacity of smoke exhaust fans based on the exhaust capacity needed to prevent the descent of the smoke below a stipulated position. The required exhaust capacity was determined based on establishing an equilibrium smoke layer position where the mass rate of smoke exhaust was equated to the mass rate of smoke being to the layer by the plume.

Codes in the U.S. and many other countries have adopted this new hazard-based approach by stipulating that the smoke layer be kept at a sufficient distance above the highest level of the means of egress to prevent a standing individual from being submerged in the smoke layer while evacuating (see Figure 1) [4,5]. This is a conservative strategy assuming that all smoke is inherently hazardous and needs to be avoided.

The equilibrium smoke layer position is dictated by the balance between the mass rate of smoke exhaust from the layer and the mass rate of smoke supply to the layer. Because smoke is predominantly composed of entrained air, the rate of smoke production can be estimated as the rate of air entrainment. There are several correlations available in the literature to estimate the rate of air entrainment [6], such as Heskestad's [7] correlations included in NFPA 92B:

$$\dot{m} = 0.071\dot{Q}_c^{1/3}z^{5/3} + .0013\dot{Q}_c \quad z > z_f \quad (1)$$

$$\dot{m} = 0.032\dot{Q}_c^{3/5}z \quad z \leq z_f \quad (2)$$

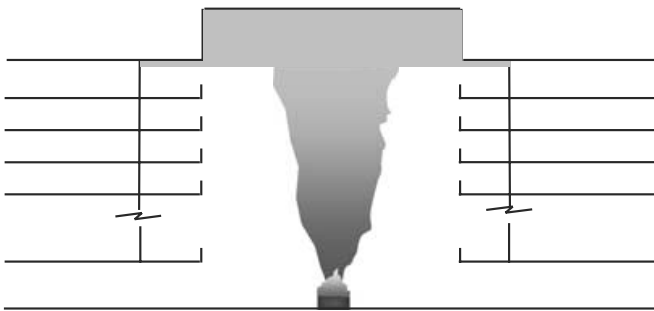


**Figure 1.** Code-specified position of smoke layer in atrium.

where

$$z_f = 0.166\dot{Q}_c^{2/5} \quad (3)$$

The smoke production rate is presented as a function of heat release rate and clear height in Figure 2, as determined by Equations (1) and (2), with the convective portion of the heat release rate assumed to be 70% of the total heat release rate, *i.e.*  $\dot{Q}_c = 0.7\dot{Q}$  [3] (other fractions of the heat release rate may be appropriate for some fuels).

If a large clear height is required, the smoke exhaust rate required will be appreciable. However, the entrained air also dilutes the smoke. Consequently, while appreciable smoke is generated, the smoke may pose little or no hazard to people or contents. Thus, providing high capacity exhaust fans will remove smoke that is appreciably diluted. Hansell and Morgan [8] suggest that for cases where the clear height is so large that the required smoke exhaust rate exceeds 200 kg/s, the design may not be cost-effective. As indicated in Figure 2, the required smoke exhaust capacity reaches 200 kg/s if the clear height ranges from 20 to 30 m for fires ranging in heat release rate from 1 to 10 MW. Limiting the exhaust rate to a maximum of 200 kg/s would reduce the cost of exhaust fans seeking to exhaust greater quantities of smoke, but would also affect other requirements, such as make-up air supply and power requirements.

A maximum effective smoke exhaust rate can be identified by conducting a hazard analysis for people or contents immersed in the residual smoke layer. The hazard analysis would need to estimate the smoke layer properties and compare the magnitude of such properties with performance criteria based on threshold damage levels. This paper outlines a method of conducting such a hazard analysis. The method is demonstrated using the

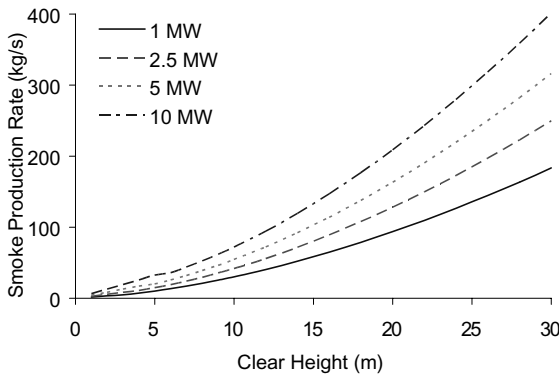


Figure 2. Smoke production rate.

200 kg/s exhaust rate proposed by Hansell and Morgan, though using 200 kg/s should not be construed as a recommended upper limit for exhaust by this author. The conditions with other exhaust rates can be examined using the method outlined in this paper.

### HAZARD LIMITS OF SMOKE

Hazard limits to determine the acceptability of a smoke management system design depend on the sensitivity of the exposed people or objects of concern. Tenability limits can be referenced where life safety is the principal concern [9,10], though a range of limits have been described in the literature. In applying the method outlined in this paper to establish a maximum effective exhaust rate, definitive tenability limits would need to be established.<sup>1</sup>

Carbon monoxide concentrations of 1000 to 8000 ppm may cause humans to become incapacitated if exposed to 1–2 min while walking or being engaged in a similar “light” activity [9]. Exposure to irradiation from a smoke layer of at least 160°C (delivering 2 kW/m<sup>2</sup>, assuming the smoke layer to be a black body) for a short duration (5 to 10 s) can cause painful skin burns. People can tolerate convective heating conditions while submerged in 100°C smoke for approximately 10 min. The noted limits of gas concentration, temperature and heat apply principally to “average” individuals. Little data is available to propose comparable limits for hyper-sensitive individuals.

Reductions in visibility have been proposed as a tenability limit even though a reduction in visibility is not self-sufficient to cause harm. A reduction in visibility makes people more susceptible to tripping over obstructions or reduce their walking speed, thereby increasing the amount of time that they are exposed to the other effects of smoke [11,12]. Previously proposed optical density limits range from 0.04 to 0.30 m<sup>-1</sup> [12–18]. The visibility of a lighted exit sign can be related to the optical density [10]:

$$S = \frac{0.43K}{D} \quad (4)$$

Estimating  $K=6$  for a back-lit exit sign, the optical density limits cited in the literature relate to a range in visibility of 9–64 m.

---

<sup>1</sup>Establishing such limits is beyond the scope of this paper.

Where exposure to electronic equipment and data storage media are of concern, temperature limits of 40°C for diskettes and 80°C for computer hardware are suggested [19]. Concentrations of 100 ppm of HCl or 1000 ppm of HF are capable of damaging electronic equipment [19].

## ESTIMATING THE HAZARD POSED BY SMOKE

Algebraic correlations, small-scale physical models, computer-based zone models and CFD models can be applied to estimate the residual hazard posed by smoke with an operating smoke management system. This paper presents a hazard assessment methodology using the algebraic correlations included in NFPA 92B [3] for equilibrium conditions.<sup>2</sup> These correlations are based on a zone model approach, where conditions in the upper layer are considered to be uniform. While these equations are developed using simplifying assumptions associated with the zone model approach and the geometry of the space, this approach is adequate to compare the influence of selected parameters on the level of hazard from fires in atria.

Parameters used to assess the hazard posed by a smoke layer are the depth (described previously) and properties of the smoke layer. The smoke layer properties of interest include temperature, gas species concentration and light obscuration (based on a reduction in visibility).

## SMOKE LAYER PROPERTIES

### Temperature

The temperature of the smoke layer can be determined by applying an energy balance [7]:

$$(1 - \chi_l)\dot{Q}_c = \dot{m}_e c_p \Delta T \quad (5)$$

At equilibrium, the mass rate of exhaust is equal to the mass rate of smoke supply to the smoke layer, *i.e.*  $\dot{m}_e = \dot{m}$ . Rearranging Equation (5):

$$\frac{\dot{m}_e}{\dot{Q}} = \lambda(1 - \chi_l) \frac{1}{c_p \Delta T} \quad (6)$$

Very limited guidance is available to select a particular value of  $\chi_l$ . Walton suggests that  $\chi_l$  ranges between 0.6 and 0.9 for relatively small spaces of near

<sup>2</sup>“Equilibrium” refers to the case where the smoke layer depth and properties remain steady.

cubic shape [20]. Most design guides for atrium smoke management conservatively assume an adiabatic smoke layer, i.e.  $\chi_1 = 0$ . Using the adiabatic assumption, predicted smoke layer temperatures are greater than would actually occur.

The heat loss fraction is expected to be dependent on the characteristics of the ceiling as well as the overall ceiling height as indicated by Hill et al. [21]. An analysis of data from recent hangar tests conducted by the US Navy [22] can be used to provide an estimate for  $\chi_1$  associated with one set of tests conducted in a tall space. In these tests, measurements from a grid of near-ceiling thermocouples can be compared to the predictions from a transient analysis of the smoke layer temperature in a curtained area near the ceiling in the tests, until smoke is observed to spill from the curtained area [23].<sup>3</sup> The smoke layer temperature is estimated as:

$$T = T_o \exp\left(\frac{(1 - \chi_1)Q}{Q_o}\right) \quad (7)$$

Rearranging Equation (7) to solve for  $\chi_1$  yields:

$$\chi_1 = \left(\frac{Q_o}{Q}\right)\left(1 - \ln\left(\frac{T}{T_o}\right)\right) \quad (8)$$

The fire sizes and heat release rates for the seven tests with JP-5 are summarized in Table 1. The ceiling height was 14.9 m and the curtained area was 7220 m<sup>2</sup>. The depth of the draft curtains was 1.5 m. The thermocouple placement is indicated in Figure 3 and Table 2. Results from Tests 1 and 7

**Table 1. Fire sources for navy tests [22].**

| Test # | Heat release rate (kW) | Pan Size       |
|--------|------------------------|----------------|
| 1      | 100                    | 0.3 × 0.3 m    |
| 2      | 500                    | 0.6 × 0.6 m    |
| 3      | 1500                   | 0.9 × 0.9 m    |
| 4      | 3000                   | 1.5 m diameter |
| 5      | 6800                   | 2.0 m diameter |
| 6      | 7700                   | 2.5 m diameter |
| 7      | 5600                   | 2.0 m diameter |

<sup>3</sup>The heat loss fraction is assumed to be independent of whether the smoke layer is varying with time or is at equilibrium. The noted temperatures were not corrected for radiation.

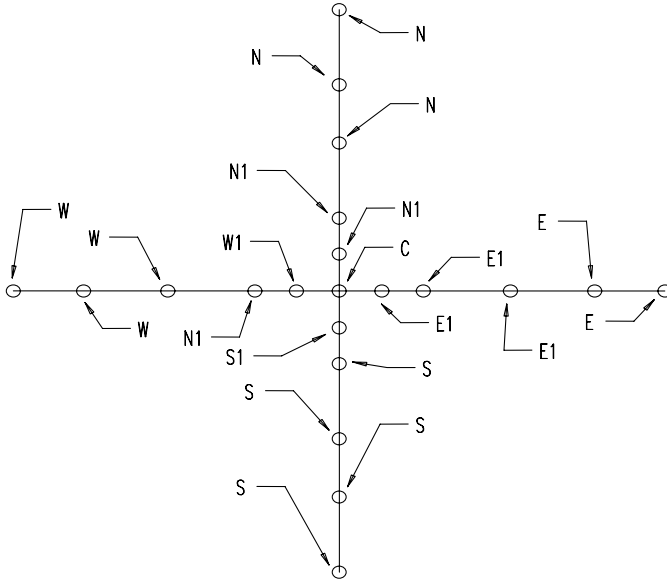


Figure 3. Position of near-ceiling thermocouples above fire.

Table 2. Placement of thermocouples – distance from center of plume [22].

| Distance From Center (m) | North | East | South | West |
|--------------------------|-------|------|-------|------|
| 1.52                     | N11   | E16  | S10   | W11  |
| 3                        | N10   | E15  | S9    | W10  |
| 6.1                      | N5    | E10  | S4    | W5   |
| 8.5                      | N2    | –    | S3    | –    |
| 9.1                      | –     | E4   | –     | W4   |
| 11.6                     | N1    | E3   | S2    | W3   |

will not be included in this assessment. In Test 1, the time for smoke filling is not reported and the draft curtains were removed in Test 7.

The average temperatures for Test 2, as one representative test are indicated in Figure 4. Results from determining  $\chi_1$  based on Equation (8) using an average temperature for all of the near-ceiling thermocouples in the test are presented in Figure 5. As indicated in the figure,  $\chi_1$  varies with time. For these tests, an approximate steady value of 0.7 for  $\chi_1$  is reasonably conservative for the purposes of estimating the smoke layer temperature and will be used in this paper as an example.

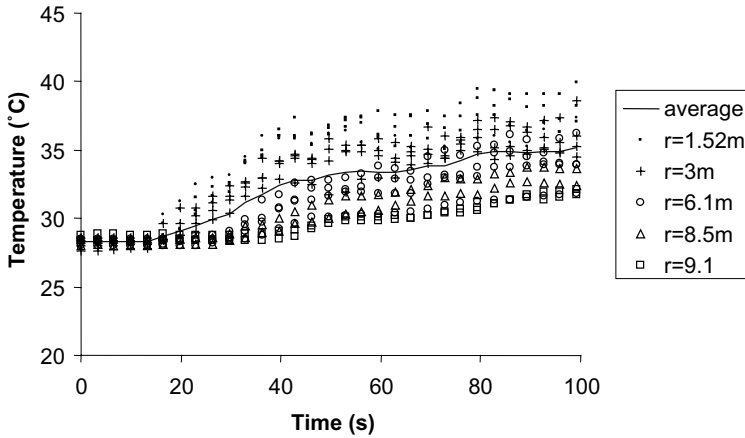


Figure 4. Near-ceiling temperatures, test 2 of navy tests.

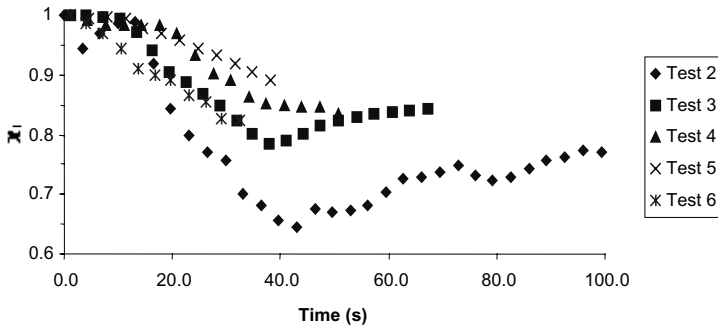
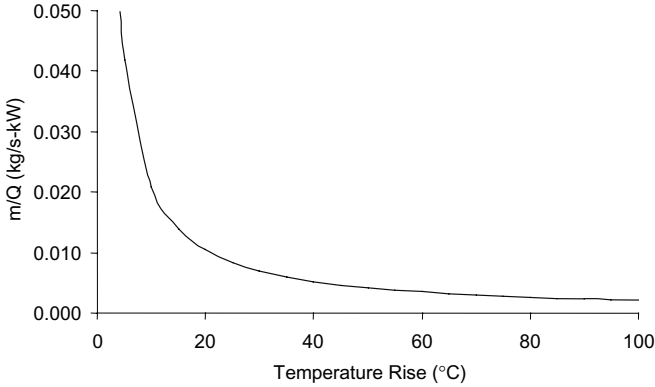


Figure 5. Estimated  $\chi_1$  from navy tests.

With the guidance for  $\chi_1$ , the temperature of a smoke layer is presented in Figure 6 for a range of mass exhaust rates. When considering a smoke management design with a mass exhaust rate of 200 kg/s, the estimated temperature rise ranges from 1 to 10°C for fire sizes between 1 and 10 MW. Doubling the exhaust rate to 400 kg/s would result in a temperature rise of 5°C for a 10 MW fire. The tenability time<sup>4</sup> for an individual immersed in a smoke layer at a temperature of 30°C (115°C above 20°C ambient) for the exhaust rate of 200 kg/s is at least 4 min [9], while that for a 78°C smoke layer temperature (associated with the exhaust rate of 400 kg/s) is 21 min.<sup>5</sup>

<sup>4</sup>In this example, tenability time is assessed as the time for incapacitation.

<sup>5</sup>As a comparison, with  $\chi_1$  of zero, the range in smoke layer temperature rise with an exhaust rate of 200 kg/s is 3.5–35°C.



**Figure 6.** Temperature rise vs mass exhaust rate and heat release rate.

### Gas Species Concentration

Conservation of mass can be applied to develop an expression for the steady state gas species concentration of the smoke layer. Losses of the species, either due to absorption by the enclosure or chemical reactions, are neglected [7].

The mass fraction of species “*i*” in the smoke layer is defined as:

$$Y_i = \frac{\dot{m}_i}{\dot{m}_e} \quad (9)$$

where the mass of species, *i*, can be determined using Equation (10):

$$\dot{m}_i = f_i \dot{m}_f = \frac{f_i \dot{Q}}{\chi_a \Delta H_c} \quad (10)$$

Substituting Equation (10) into Equation (9) and replacing  $Y_i$  with  $C_i$ , the volumetric proportion of the gas species (in terms of ppm), yields:

$$\frac{\dot{m}_e}{\dot{Q}} = \frac{f_i}{\chi_a \Delta H_c} \frac{10^6}{C_i} \frac{MW_{\text{air}}}{MW_i} \quad (11)$$

The term  $f_i/\chi_a \Delta H_c$  is referred to as the gas fuel parameter [24]. This parameter is fuel dependent and varies with the burning mode, ventilation conditions and operation of sprinklers. The CO fuel parameter is provided in Table 3 for selected fuels. The specific fuels are selected to provide a wide range of values of the parameter [25]. The yield fractions,  $f_i$ , used to

**Table 3. CO and visibility fuel parameters for selected fuels.**

| Fuel                   | $f_{CO}$<br>(kg CO/kg<br>fuel) | $D_m$<br>(m <sup>2</sup> /g) | $\chi_a \Delta H_c$<br>(kJ/g) | $f_{CO}/\chi_a \Delta H_c$<br>(kg/kJ) $\times 10^{-6}$ | $D_m/\chi_a \Delta H_c$<br>(m <sup>2</sup> /kJ) $\times 10^{-3}$ |
|------------------------|--------------------------------|------------------------------|-------------------------------|--|--|
| Ethane                 | 0.001                          | 0.303                        | 45.7                          | 0.0219   | 6.63   |
| Propane                | 0.005                          | 0.112                        | 43.7                          | 0.114  | 2.57   |
| Heptane                | 0.010                          | 0.297                        | 41.2                          | 0.243  | 7.21   |
| Styrene                | 0.065                          | 0.899                        | 27.8                          | 2.34   | 3.23   |
| Red Oak                | 0.004                          | 0.0576                       | 12.4                          | 0.323  | 4.64   |
| Douglas fir            | 0.004                          | 0.0636                       | 13.0                          | 0.308  | 4.89   |
| Pine                   | 0.005                          | 0.0535                       | 12.4                          | 0.403  | 4.31   |
| Polymethylmethacrylate | 0.010                          | 0.157                        | 24.2                          | 0.413  | 6.47   |
| Polyethylene           | 0.024                          | 0.382                        | 38.4                          | 0.625  | 9.95   |
| Polypropylene          | 0.024                          | 0.384                        | 38.6                          | 0.622  | 9.95   |
| Polystyrene            | 0.060                          | 0.806                        | 27.0                          | 2.22   | 29.9   |
| Polystyrene foam       | 0.058–0.065                    | 0.734–0.966                  | 24.6–25.9                     | 2.32–2.54  | 29.9–37.3  |
| Nylon                  | 0.038                          | 0.382                        | 27.1                          | 1.40   | 14.1   |
| Polyvinylchloride      | 0.063                          | 0.709                        | 5.7                           | 11.2   | 124  |

determine the gas fuel parameter values included in Table 3 apply to well-ventilated, flaming fires of relatively small samples [25]. These values are applicable for smoke hazard analysis from atrium fires because the greatest threat for fires in the atria will be posed by well-ventilated, flaming fires. Different yield fractions would apply to fires in connected spaces, if oxygen-depleted conditions occur.

For the proposed maximum mass exhaust rate of 200 kg/s, the steady state smoke layer CO concentration for a fire involving a particular fuel is a function of the heat release rate only.

$$C_i = 5000 \frac{f_i}{\chi_a \Delta H_c} \frac{MW_{air}}{MW_i} \dot{Q} \quad (12)$$

Figure 7 presents the results of applying Equation (12) for heat release rates up to 10 MW. The maximum CO concentration expected for the range of fire sizes up to 10 MW is approximately 100 ppm for all fuels noted in Table 3 except polyvinyl chloride<sup>6</sup>. This concentration of CO would have little impact on average people if exposed for several hours [9].

<sup>6</sup>The situation is only significant for polyvinyl chloride if it is the only fuel being consumed to create a fire with a heat release rate of 1–10 MW.

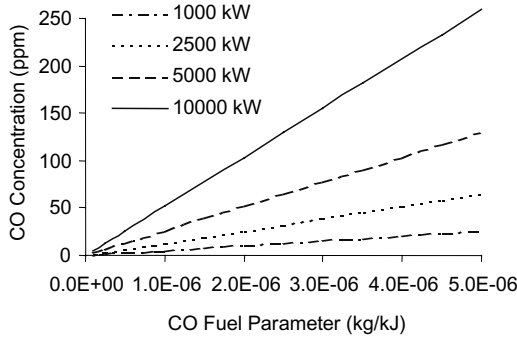


Figure 7. CO concentration for a mass exhaust rate of 200 kg/s.

**Optical density**

The optical density of the smoke layer is determined assuming all of the fire-generated particles are transported to the layer by the plume and accumulate in the smoke layer. Plating out on enclosure surfaces and changes due to smoke aging are neglected [7]. The optical density can be related to the mass optical density, fuel mass loss rate and volumetric exhaust capacity:

$$D = \frac{D_m \dot{m}_f}{\dot{V}_e} \tag{13}$$

Substituting for the mass burning rate in terms of the heat release rate and heat of combustion, replacing the volumetric exhaust rate with the mass exhaust rate and using Equation (4) to replace the optical density with  $K=6$  for back-lit exit signs:

$$\frac{\dot{m}_e}{\dot{Q}} = \frac{\rho_o}{0.43K} \frac{D_m}{\chi_a \Delta H_c} S \tag{14}$$

As with the gas fuel parameter, a visibility fuel parameter is defined as,  $D_m/\chi_a \Delta H_c$ , that is dependent on the fuel, burning mode, ventilation conditions and operation of sprinklers. The mass optical density can vary by several orders of magnitude for different ventilation conditions [25]. The visibility fuel parameter is provided in Table 3 for selected fuels that again span a wide range of values of the parameter [25,26]. The values of  $D_m$  selected for the fuels apply to well-ventilated, flaming fires. Solving

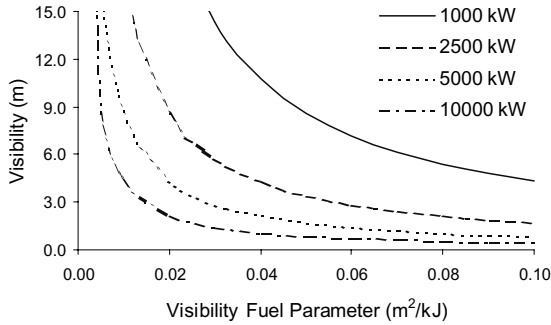


**Figure 8.** Visibility through smoke for a mass exhaust rate of 200 kg/s.

Equation (14) for the visibility distance for a mass exhaust rate of 200 kg/s, yields:

$$S = \frac{200}{\dot{Q}} \left[ \frac{\rho_o}{0.43K} \frac{D_m}{\chi_a \Delta H_c} \right]^{-1} \quad (15)$$

The relationship of visibility to heat release rate and the visibility fuel parameter for a mass exhaust rate of 200 kg/s is presented in Figure 8. Considering that the visibility fuel parameter is at least 0.030 m<sup>2</sup>/kJ for polystyrene foam and polyvinyl chloride among the fuels noted in Table 3, the visibility through a smoke layer may be reduced significantly if only 200 kg/s of exhaust is provided<sup>7</sup>.

### COMPARISON OF HAZARD POSED BY SMOKE LAYER PROPERTIES

Relationships between the three smoke layer properties (temperature, gas species concentration and optical density) can be formulated and used to assess which of the three properties is likely to dictate the acceptability of a particular design. The CO concentration is related to temperature rise in Equation (16), derived by equating Equations (5) and (10):

$$C_{CO} = 0.45 \times 10^6 \frac{f_i}{\chi_a \Delta H_c} \Delta T \quad (16)$$

<sup>7</sup>As noted for the calculations of CO, the visibility conditions generated for polystyrene foam and polyvinyl chloride apply if the burning fuel providing the assumed heat release rate is comprised solely of these polymers.

As indicated in Equation (16) and Figure 9, the CO concentration is linearly proportional to the temperature rise. For CO fuel parameter values of  $2.5 \times 10^{-6}$  kg/kJ or less (encompassing all of the fuels included in Table 3 except for polyvinylchloride), the CO concentration indicated in Figure 9 is modest if the temperature rise is modest. As such, for situations where ordinary sprinklers (operating temperature of  $74^\circ\text{C}$ ) are not expected to activate, i.e. for a temperature rise of approximately  $50^\circ\text{C}$  or less, the hazard due to CO concentration in the smoke layer is minimal. The exception would involve fires involving fuels consisting solely of polyvinylchloride.

Similarly, a relationship between visibility and temperature rise, expressed as Equation (17) is obtained by equating Equations (5) and (14). Visibility and CO concentration can be related by equating Equations (10) and (14).

$$S = \frac{0.43K}{\rho_o} \frac{D_m}{\chi_a \Delta H_c} \left( \frac{\lambda}{1 - \chi_l} \right) \frac{1}{c_p \Delta T} = 5.0 \frac{D_m}{\chi_a \Delta H_c} \frac{1}{\Delta T} \quad (17)$$

$$S = \frac{f_i}{D_m} \frac{0.43 \times 10^6 K}{\rho_o} \frac{MW_{\text{air}}}{MW_{\text{CO}} C_i} \frac{1}{C_i} = 0.37 \times 10^6 \frac{f_i}{D_m} \frac{1}{C_{\text{CO}}} \quad (18)$$

The resulting relationships indicate that the visibility is inversely proportional to the temperature rise and CO concentration.<sup>8</sup> The results of

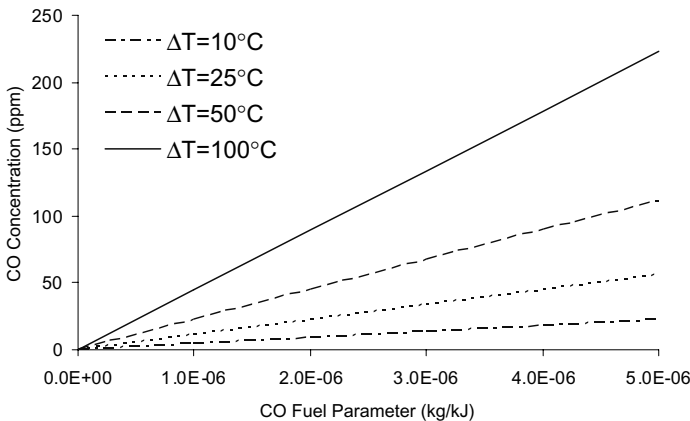
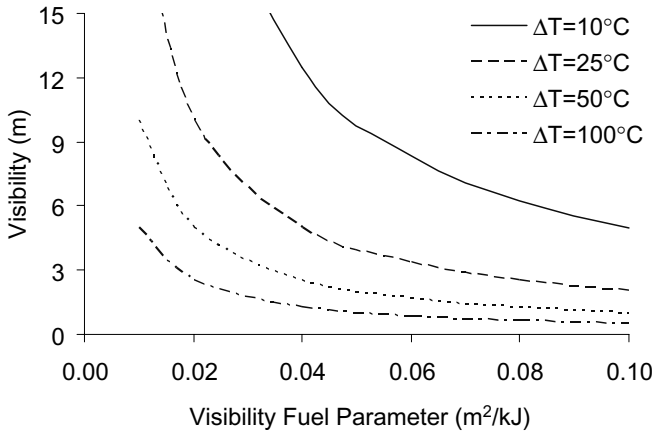


Figure 9. Temperature rise vs CO concentration in smoke layer.

<sup>8</sup>Optical density is linearly proportional to the temperature rise and CO concentration.

applying Equations (17) and (18) are presented in Figures 10 and 11. In Figure 10, the visibility is plotted for a range of values of the visibility fuel parameter and temperature rises between 10 and 100°C. In Figure 11, the relationship of the visibility is depicted as a function of a fuel dependent parameter consisting of the ratio of the yield fraction and mass optical density. Being that the ratio of  $f_i/D_m$  ranges from  $10^{-6}$  to  $10^{-4}$  for the fuels listed in Table 3, the visibility reduction is substantial, even though the



**Figure 10.** Visibility vs temperature rise in smoke layer.

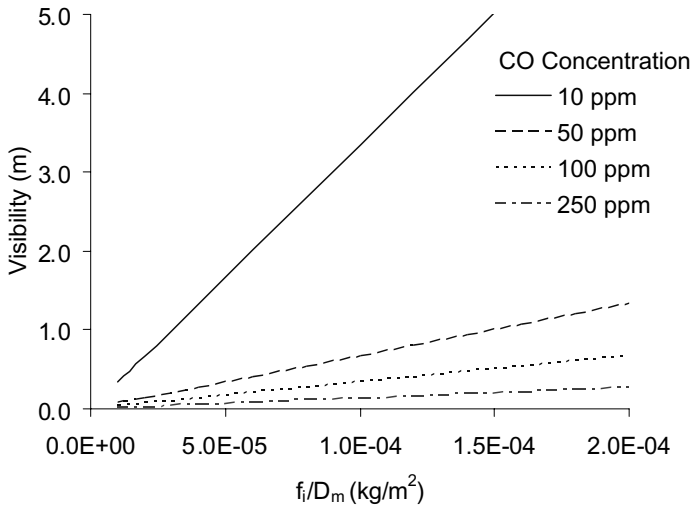


**Figure 11.** Visibility vs CO concentration in smoke layer.

hazard due to temperature or CO concentration is relatively minor for the range of fire sizes considered.

### RECOMMENDATION OF A MAXIMUM EXHAUST RATE

Having noted that visibility is the governing criterion, an analysis of the largest beneficial exhaust rate can be conducted. The visibility fuel parameter for most of the fuels listed in Table 3 is less than  $0.03 \text{ m}^2/\text{kJ}$ . Substituting  $0.03 \text{ m}^2/\text{kJ}$  for the visibility fuel parameter in Equation (14), mass exhaust rate can be expressed in terms of the minimum visibility distance and heat release rate as:

$$\dot{m}_e = 0.014S\dot{Q} \quad (19)$$

The mass exhaust rate to maintain a particular level of visibility for fire sizes ranging from 1 to 10 MW involving fuels with a visibility fuel parameter of  $0.03 \text{ m}^2/\text{kJ}$  is presented in Figure 12. With a mass exhaust rate of 200 kg/s, a visibility of 3 m can be maintained for fires with heat release rates up to 4.8 MW. However, with an exhaust rate of 200 kg/s, the visibility is proportionally less for larger fires. For example, the visibility would be limited to a distance of 1.4 m for a heat release rate of 10 MW.

The results presented in Figure 12 are based on a visibility fuel parameter of  $0.03 \text{ m}^2/\text{kJ}$ , which is intended to represent an upper limit for fuels involved in well-ventilated, flaming fires. As such, the fire must involve only fuels with a visibility fuel parameter of this magnitude, possibly resulting in this analysis appreciably overestimating the smoke conditions.

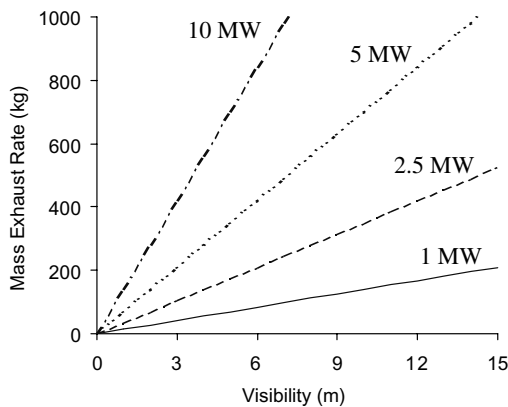


Figure 12. Mass exhaust rate to maintain visibility (visibility fuel parameter =  $0.03 \text{ m}^2/\text{kJ}$ ).

## SUMMARY

A hazard analysis method using algebraic equations has been developed to estimate the properties of the smoke layer at equilibrium with an operating smoke management system. This methodology has been developed to permit the analysis of the benefits provided by very large exhaust quantities often intended to maintain very large clear heights. Smoke exhaust rates in excess of 200 kg/s had been previously proposed as having little additional benefit over the conditions provided by an exhaust rate of 200 kg/s.

Based on the analysis conducted, visibility reduction appears to be the most demanding parameter for flaming, well-ventilated fires. The estimated visibility is reduced to 3 m or less even though the temperature rise and CO concentration are relatively modest for smoke exhaust rates of 200 kg/s. Compared to the reduction in visibility, temperature rise and CO concentration are relatively modest for a wide range of fuels and fire sizes.

Prior to developing any firm conclusions on the opinion that 200 kg/s is a maximum effective smoke exhaust rate, the following questions need to be addressed:

- What is a reasonable design value for the gas and visibility fuel parameters for a mixture of fuels resident in atria, covered malls and similar spaces? The previous analysis assumed that the entire fire involved a single fuel with a characteristic value for the parameters.
- Can consensus be achieved on a tenability limit for visibility?

## NOMENCLATURE

- $A$  = floor area of atrium ( $m^2$ )  
 $C_i$  = concentration of gas species “ $i$ ” (ppm)  
 $C_{CO}$  = concentration of CO (ppm)  
 $c_p$  = specific heat of ambient air (1.005 kJ/kg K)  
 $D$  = optical density ( $m^{-1}$ )  
 $D_m$  = mass optical density ( $m^2/kg$ )  
 $f_i$  = yield fraction of species “ $i$ ” (kg of species “ $i$ ” per kg of fuel consumed)  
 $H$  = ceiling height of atrium (m)  
 $\Delta H_c$  = heat of combustion (kJ/kg)  
 $K$  = constant, depending on target being viewed, e.g. = 6 for lighted signs  
 $MW_{air}$  = molecular weight of air (kg/mol)  
 $MW_{CO}$  = molecular weight of CO (kg/mol)  
 $MW_i$  = molecular weight of species “ $i$ ” (kg/mol)

- $\dot{m}$  = mass rate of air entrainment (kg/s)  
 $\dot{m}_e$  = mass exhaust rate (kg/s)  
 $\dot{m}_f$  = mass loss rate of fuel (kg/s)  
 $\dot{m}_i$  = mass generation of species “ $i$ ” (kg/s)  
 $Q$  = total heat generated by fire, =  $\dot{Q}t$  (kJ)  
 $Q_o$  = internal energy of smoke layer, =  $\rho_o c_p T_o A(H-z)$   
 $\dot{Q}$  = heat release rate of fire (kW)  
 $\dot{Q}_c$  = convective portion of heat release rate of fire (kW)  
 $S$  = visibility distance to exit sign (m)  
 $T$  = temperature of smoke layer ( $^{\circ}\text{C}$ )  
 $T_o$  = ambient temperature ( $^{\circ}\text{C}$ )  
 $\Delta T$  = temperature rise of smoke layer ( $^{\circ}\text{C}$ )  
 $Y_i$  = mass fraction of gas species “ $i$ ” (kg of species “ $i$ ” per kg of smoke)  
 $z$  = height above top of fuel to smoke layer interface (m)  
 $z_f$  = average flame height (m)  
 $\chi_a$  = combustion efficiency  
 $\chi_l$  = heat loss fraction from smoke to enclosure  
 $\lambda$  = ratio of heat released convectively to the total heat release rate  
 $\rho_o$  = density of ambient air ( $1.2 \text{ kg/m}^3$ )

## REFERENCES

1. NFPA, “Life Safety Code,” NFPA 101, Quincy, MA, 1988.
2. Milke, J. A., “Smoke Management for Covered Malls and Atria,” *Fire Technology*, Vol. 26, No. 3, 1990, pp. 223–243.
3. NFPA, “Guide for Smoke Management Systems in Malls, Atria, and Large Areas,” NFPA 92B, Quincy, MA, 2000.
4. CIBSE, “Relationships for Smoke Control Calculations,” TM 19, Chartered Institution of Building Services Engineers, London, 1999.
5. NFPA, “Life Safety Code,” NFPA 101, Quincy, MA, 2000.
6. Beyler, C. L., “Fire Plumes and Ceiling Jets,” *Fire Safety J.*, Vol. 11, No. 1,2, 1986, pp. 53–76.
7. Heskestad, G., “Engineering Relations for Fire Plumes,” SFPE TR 82-8, SFPE, 1982.
8. Hansell, G. O. and Morgan, H. P., “Design Approaches for Smoke Control in Atrium Buildings,” Building Research Establishment, 1994.
9. Purser, D. A., “Toxicity Assessment of Combustion Products,” SFPE Handbook of Fire Protection Engineering, 3rd Edition, P.J. DiNenno ed., NFPA 2002.
10. Klote, J. H. and Milke, J. A., “Principles of Smoke Management, American Society of Heating, Refrigerating and Air-Conditioning Engineers, 2002.
11. Jin, T., “Irritating Effects of Fire Smoke on Visibility,” *Fire Science and Technology*, Vol. 5, No. 1, 1985, pp. 79–90.
12. Jin, T., “Visibility Through Fire Smoke,” *J. of Fire and Flammability*, Vol. 9, 1978, pp. 135–155.

13. Tamura, G. T., "Smoke Movement and Control in High-rise Buildings," NFPA, 1994.
14. Kawagoe, K. and Saito, H., "Measures to Deal with Smoke Problems Caused by Fire," J. of Japan Society for Safety Engineering, Vol. 6, No. 7, 1967, pp. 108-114.
15. Wakamatsu, T., "Calculation of Smoke Movement in Buildings," Building Research Institute, Research Paper No. 34, 1968.
16. Los Angeles Fire Department, "Operation School Burning," No. 2, NFPA, 1961.
17. Rasbash, D. J., "Smoke and Toxic Products Produced at Fires," Transactions and Journal of Plastics Institute, 1967, pp. 55-61.
18. Malhotra, H. L., "Movement of Smoke on Escape Routes," Instrumentation and Effect of Smoke on Visibility, FR Notes 651, 652, 653, Borehamwood, UK, 1967.
19. NFPA, "Standard for the Protection of Electronic Computer/Data Processing Equipment," NFPA 75, 1999.
20. Walton, W. D., "ASET-B: A Room Fire Program for Personal Computers," NBSIR 85-3144, National Bureau of Standards, 1985.
21. Hill, S. M., Quintiere, J. G. and Milke, J. A., "Analysis of Smoke Layer Properties During the Transient Filling Period in Atria and Large-Volume Spaces," Proceedings: 2nd International Conference on Fire Research and Engineering, Bethesda, MD, SFPE, 1998, pp. 463-474.
22. Gott, J. E., Lowe, D. L., Notarianni, K. A. and Davis, W. D., "Analysis of High Bay Hangar Facilities for Fire Detector Sensitivity and Placement," NIST TN 1423, National Institute of Standards and Technology, 1997.
23. Milke, J. A. and Mowrer, F. W., "A Design Algorithm for Smoke Management Systems in Atria and Covered Malls," Report FP 93-04, Report to American Society of Heating, Refrigerating and Air-Conditioning Engineers, University of Maryland, 1993.
24. Mowrer, F. W., "Enclosure Smoke Filling and Management with Mechanical Ventilation," Fire Technology, Vol. 38, No. 1, 2002, pp. 33-56.
25. Tewarson, A., "Generation of Heat and Chemical Compounds in Fires," SFPE Handbook of Fire Protection Engineering, 3rd Edition, P.J. DiNenno ed., NFPA, 2002.
26. Mulholland, G., "Generation of Heat and Chemical Compounds in Fires," SFPE Handbook of Fire Protection Engineering, 3rd Edition, P.J. DiNenno ed., NFPA, 2002.